Separation Science and Technology
Publication details, including instructions for authors and subscription information:
http://www.informaworld.com/smpp/title~content=t713708471

Equilibrium and Fixed Bed Adsorption of 1-Butene, Propylene and Propane Over 13X Zeolite Pellets

Nabil Lamia[ab]; Luc Wolff[b]; Philibert Leflaive[b]; Damien Leinekugel-Le-Cocq[b]; Pedro Sá Gomes[a]; Carlos A. Grande[a]; Alírio E. Rodrigues[a]
[a] Laboratory of Separation and Reaction Engineering (LSRE), Faculty of Engineering, Department of Chemical Engineering, University of Porto, Porto, Portugal [b] IFP-Lyon Process Development and Engineering Division, Institut Français du Pétrole, Vernaison, France

To cite this Article Lamia, Nabil , Wolff, Luc , Leflaive, Philibert , Leinekugel-Le-Cocq, Damien , Gomes, Pedro Sá , Grande, Carlos A. and Rodrigues, Alírio E.(2008) 'Equilibrium and Fixed Bed Adsorption of 1-Butene, Propylene and Propane Over 13X Zeolite Pellets', Separation Science and Technology, 43: 5, 1124 — 1156
To link to this Article: DOI: 10.1080/01496390801888136
URL: http://dx.doi.org/10.1080/01496390801888136

Separation Science and Technology, 43: 1124–1156, 2008

ISSN 0149-6395 print/1520-5754 online
DOI: 10.1080/01496390801888136

Equilibrium and Fixed Bed Adsorption of 1-Butene, Propylene and Propane Over 13X Zeolite Pellets

Nabil Lamia,[1,2] Luc Wolff,[2] Philibert Leflaive,[2] Damien Leinekugel-Le-Cocq,[2] Pedro Sá Gomes,[1] Carlos A. Grande,[1] and Alírio E. Rodrigues[1]

[1]Laboratory of Separation and Reaction Engineering (LSRE), Faculty of Engineering, Department of Chemical Engineering, University of Porto, Porto, Portugal
[2]Institut Français du Pétrole, IFP-Lyon Process Development and Engineering Division, Vernaison, France

Abstract: Propylene-propane separation is one of the most difficult and demanding energetic operation currently practiced using cryogenic distillation. Extensive studies on various alternatives showed that cyclic adsorption processes, and particularly pressure swing adsorption (PSA), might be an option to replace the traditional distillation. In spite of the promising results of the PSA process, much attention is currently being paid to the simulated moving bed technology (SMB) for gas-phase separations. The ingenious principle of this process is based on the choice of an adequate adsorbent-desorbent couple. Thus, in the present work 1-butene has been studied as an interesting desorbent to displace adsorbed propylene-propane mixture on 13X zeolite. The measurements of pure 1-butene adsorption isotherms over 13X zeolite were performed with a gravimetric experimental device for pressure ranging from 0 to 110 kPa and at temperature of 333, 353, 373, and 393 K. The experimental adsorption data were correlated using Toth model. The heat of adsorption at zero coverage and the maximum loading capacity of 1-butene were found to be 54.4 kJ/mol and 2.10 mol/kg, respectively. The adsorption and desorption of 1-butene on 13X zeolite packed on a fixed bed initially saturated either by a propane-propylene mixture or a pure C_3

Received 17 August 2007, Accepted 6 December 2007
Address correspondence to Alírio E. Rodrigues, Laboratory of Separation and Reaction Engineering (LSRE), Faculty of Engineering, Department of Chemical Engineering, University of Porto, Rua Dr. Roberto Frias s/n, 4200-465, Porto, Portugal. Tel.: 351 22 5081671; Fax: 351 22 5081674; E-mail: arodrig@fe.up.pt

hydrocarbon has been studied. The performance of 1-butene has been compared with isobutane that was previously proposed to be a highly effective desorbent for C_3H_6/C_3H_8 separation. A model based on a double LDF approximation for the mass transfer combined to a heterogeneous energy balance taking into account a variable velocity of the gaseous bulk phase, has been used to describe the breakthrough curves obtained experimentally at 373 K and 110 kPa.

Keywords: 1-Butene, 13X Zeolite, adsorption equilibrium, fixed bed adsorption experiments

INTRODUCTION

The separation of propylene from mixtures with propane is a very important and large volume operation in the petrochemical industry. Steam cracking and fluid catalytic cracking are among the most common and large scale processes leading to the propane-propylene mixture. The recovery of propylene from this mixture has a high commercial significance to the chemical industry, and particularly for the production of polypropylene. Presently, the separation of propane-propylene mixture is practiced by fractional cryogenic distillation. The very low relative volatility between the two components (1) makes this operation difficult and excessively energy consuming. As a consequence of the large size of the columns containing over 150 trays with a high reflux ratio, several alternatives have been investigated (2). Some of the most promising alternatives to perform this separation in a more efficient and cost-effective way involve the use of adsorbents that exploit their ability to adsorb some of the components selectively (3–6). This has paved the way for a number of cyclic adsorption processes such as pressure or vacuum swing adsorption (PSA/VSA) technologies (7–9). In these processes the mixture is first passed through a fixed bed of an adsorbent material under conditions where one or more of the components are selectively removed. The loaded material is then exposed to a lower pressure environment where the adsorbed gases are released and recovered at a higher purity level. The latest results reported by Grande and Rodrigues (10) showed that very high propylene purity can be obtained with an important recovery. Although the PSA process is in the way to be used in refineries, it appeared recently that other cyclic adsorption schemes, such as the simulated moving bed (SMB), could succeed in separating olefin/paraffin mixtures with higher recovery and productivity.

The SMB technology was introduced in the late 1950s and has mainly been applied for liquid-phase separation to very large-scale production in the petrochemical industry (11, 12). The main idea of this process is to simulate a continuous countercurrent flow of the fluid and of the solid adsorbent by a synchronous port shifting of the different inlets and outlets in a multi-column unit (13). The key advantage of such a process is the high-mass-transfer efficiency of this countercurrent gas-solid contact

allowing a more efficient use of the sorbent. The implementation of a conventional SMB for gas separation is based not only on the choice of a good solid adsorbent but on the selection of an efficient desorbent as well. Recent interest for gas-phase separation using the SMB process led to the emergence of cycle where the desorption steps are not carried out with a desorbent (14–18). Thus, the aim of this work is to find out an adsorbent which can be combined to an appropriate desorbent in order to carry out the gas phase separation of C_3 olefin from paraffin with a classical SMB cycle.

Different types of adsorbents have been attempted for propylene-propane separation up to various degrees of success. Some of the most common adsorbents tested for separating propylene from a mixture containing propane are zeolite type. It is worth pointing out that propylene is smaller in cross-section than propane, so it is more readily sorbed into pores of any zeolite. In the 4A zeolite (19, 20), propylene is sorbed into the pores while propane is virtually entirely excluded. Furthermore, the diffusion of propylene into and out of the zeolite pores is so slow that the separation is impractical from an industrial standpoint. Da Silva and Rodrigues reported that 13X zeolite presents a high loading capacity and low mass-transfer resistance (21) and confirmed Järvelin's work (22–24) indicating that a larger-pore 13X zeolite would work well for propane/propylene separation. Currently, a number of new π-complexation adsorbents have been studied for olefin/paraffin separations (25). Those materials have nevertheless a rather low loading capacity. In accordance with the choice made in a previous work (26) and in view of kinetic behavior, zeolite 13X was the solid adsorbent adopted for this study. A noteworthy feature distinguishing this study from the previous one is the discovery of a new desorbent, i.e. 1-butene, which could be as interesting as isobutane for displacing propane and propylene from the adsorbent bed. Because adsorption data of 1-butene over 13X zeolite are scarce, equilibrium isotherms of this C_4 olefin over 13X zeolite have been measured with a gravimetric method at a temperature ranging from 333 K to 393 K and a pressure up to 110 kPa. To make sure that the preferred desorbent is able to displace propane as well as propylene from the molecular sieve, breakthrough experiments were carried out at 373 K and 110 kPa in a laboratory-scale fixed bed column with a feed flowrate of 1.0 SLPM (standard liters per minute at 273.15 K and 1.01325×10^{-5} Pa). In addition, these fixed-bed experiments allowed to see if 1-butene is easily displaceable from the adsorbent, so that the molecular sieve could be reused in the process. Further experiments were conducted in the same operating conditions with a column fully saturated with either 1-butene or isobutane, and then desorbed from the bed by passing a mixture of propane-propylene in order to determine which one is the more efficient desorbent. It should be noted that both 1-butene and isobutane in combination with zeolite 13X have been presented in a pending patent as two possible desorbent/adsorbent couples for propane/propylene separation by simulated moving bed (27).

The dynamics of multicomponent adsorption in a fixed bed with bidisperse particles was studied as a preliminary work to a SMB model. In the mathematical model proposed in this study to describe the breakthrough curves obtained experimentally, detailed mass and energy balances were developed for a nonisothermal and nonadiabatic fixed bed adsorber in which a variable velocity of the bulk phase along the unit is taken into account.

EXPERIMENTAL SECTION

Materials

The adsorbent used in this study is 13X zeolite in extrudate form manufactured by CECA (France). Some representative properties of the adsorbent are reported in Table 1. The average crystal size of the sample was obtained by scanning electron microscopy (SEM). The 13X zeolite pore structure consists of sodalite cages arranged in such a way that large supercages are accessible through 7.2 Å windows.

The propane, propylene, and 1-butene used in this work were research-grade reagents, provided by Air Liquide (France). The purity of sorbate gases was N24 for propylene (>99.4%), N35 for propane (>99.95%) and N20 for 1-butene (>99.0%), while the purity of nitrogen used as an inert gas during the regeneration procedure was 99.995 mol% pure. All the adsorbates have a molecular diameter of less than 5.0 Å, i.e., a critical diameter smaller than the window size of the zeolite cavities.

Table 1. Physical properties of 13X zeolite and characteristics of the fixed-bed column

Adsorbent		
Extrudate radius	R_p	0.8 mm
Crystal radius	r_c	1.0 μm
Macropore radius	r_p	0.17 μm
Pellet density	ρ_p	$1357\ \text{kg} \cdot \text{m}^{-3}$
Pellet porosity	ε_p	0.395
Solid specific heat	$\hat{C}_{ps}$	$920\ \text{J} \cdot \text{kg}^{-1} \cdot \text{K}^{-1}$
Fixed-bed column		
Bed radius	R_w	$1.07\ 10^{-2}$ m
Effective bed length	L	0.84 m
Bed porosity	ε_b	0.39
Bulk density	ρ_b	$820\ \text{kg} \cdot \text{m}^{-3}$
Wall density	ρ_w	$8238\ \text{kg} \cdot \text{m}^{-3}$
Wall specific heat	$\hat{C}_{pw}$	$500\ \text{J} \cdot \text{kg}^{-1} \cdot \text{K}^{-1}$

Gravimetric Measurements of Adsorption Equilibrium

Pure gas adsorption measurements were performed on a Rubotherm magnetic suspension balance (MSB) (Bochum, Germany). Details of the equipment and the operating procedure have been described in a previous work (26). Prior to adsorption, the zeolite sample was weighed and introduced in the microbalance basket to undergo a pretreatment, i.e., to be activated. To perform this activation, the solid adsorbent was heated under vacuum from ambient temperature up to 593 K with a temperature ramp of $2\ K \cdot min^{-1}$. The sample was maintained at this temperature and 1 mbar during at least 10 hours. Once the activation was accomplished, the system was cooled down to the measurement temperature. It is worth noting, that the measuring cell was thermostated by an electrical heating device and highly accurate transducers were used to measure pressure and temperature. Thereafter, the pure component sorptive gas was fed step by step through tubing equipped with valves, from the gas cylinder to the MSB. The weight gained by the adsorbent was transmitted by magnetic suspension coupling from a closed and pressure-proof metal container to an external microbalance. Weight differences and the pressure increments were recorded with a computer. Single-adsorption equilibrium isotherms were measured at four temperatures (333, 353, 373, and 393 K) at pressure up to 110 kPa.

Fixed Bed Adsorption Experiments

Fixed bed adsorption studies were conducted to evaluate the effectiveness of 1-butene to displace propylene, propane and their mixture from 13X zeolite. Experiments were carried out in a 2.14×10^{-2} m I.D., 0.84 m length stainless steel column packed with 13X zeolite. Fixed-bed column properties are given in Table 1. The remaining void volume at both ends of the column was filled with glass beads in order to properly distribute the inlet flow along the bed and to avoid a too large void volume at the end. The column was then placed inside a convective furnace equipped with PID temperature controllers. Two Omega type K thermocouples were inserted axially in the column, one near the middle of the bed measuring the gas temperature, and the other at the top, measuring the wall column temperature. At the inlet of the column, the flow rate was controlled with a mass flow controller to get constant flow. The adsorption pressure was adjusted with a backpressure regulator (Bronkhorst, Holland). A Chromopack CP9001 gas chromatograph equipped with a FID detector was employed for analysing propane, propylene and 1-butene at the bed exit, using ethane as an external reference flow. The GC was coupled with an automatic valve sampling system containing 12 loops of 10 μl. Detailed information about the experimental installation are presented elsewhere (26). Prior to the experiments, the adsorbent bed is subjected to an activation by purging it with nitrogen overnight from ambient temperature to 593 K.

THEORETICAL SECTION

Adsorption Equilibrium

A number of equilibrium isotherm models can be used to fit experimental equilibrium data (28). In this work Toth model (29) was chosen to describe our experimental isotherms. Being a three-adjustable-parameter model, this equation is more efficient than the Langmuir's one for fitting most of the adsorption data. On the other hand, compared with other thermodynamics models it gives, with great simplicity, a quantitative description of the observed equilibriums. The Toth equation was applied in the following form:

$$q_i = q_{m,i} \frac{b_i P}{(1 + (b_i P)^{k_i})^{1/k_i}} \tag{1a}$$

and

$$b_i = b_{i,0} \exp\left(\frac{-\Delta H_i}{\Re T}\right) \tag{1b}$$

where q_i and $q_{m,i}$ are the absolute amount adsorbed and the maximum amount adsorbed of the ith component, ΔH_i is the isosteric heat of adsorption at zero loading, b is the affinity parameter of the pure component i for the solid sorbent, and $k_i = A_i + D_i T$ is the dimensionless solid heterogeneity parameter (30).

There are several ways to evaluate the precision of a fit on a set of experimental data. A commonly used parameter for adsorption isotherms is the average relative error (ARE), defined as follows:

$$\text{ARE} = \frac{100}{N} \times \sum \frac{|q_{exp} - q_{sim}|}{q_{\text{exp}}} \tag{2}$$

where N is the number of data points, q_{exp} and q_{sim} are the experimental and the calculated amount adsorbed, respectively.

Mathematical Model for Fixed Bed Adsorption

To describe the behavior of 1-butene in presence of propane, propylene and their mixture in a fixed bed adsorber, a dynamic model was developed. The adsorption system considered is a nonisothermal and nonadiabatic column packed with extrudates of 13X zeolite initially saturated either with an inert gas or a sorbate species. The model is derived from the mass and energy balances, including the following assumptions:

1) The adsorbent particles have a bidisperse porous structure containing macropores and micropores;
2) The gas phase follows the ideal gas law;

3) The pressure is constant;
4) The flow pattern is described using the axially dispersed plug flow model;
5) Mass, temperature and velocity gradients are negligible in the radial direction;
6) The mass transfer rate inside the solid, at the pellet and crystal level, is represented using a linear driving force model (LDF);
7) The adsorption equilibrium is described by multicomponent Toth model.

On this basis, the mass balance equations were written as follows.

Component Mass Balance in the Bulk Fluid

Plug flow model with axial dispersion is used to describe the bulk phase flow through the adsorption column. Axial dispersion coefficients are supposed to be the same for all components. The mass balance for the *i*th component in the bulk gas phase, including axial dispersion and variable velocity along the bed axis, is (31):

$$\frac{\partial C_i}{\partial t} = \frac{\partial}{\partial z}\left(D_{ax} C \frac{\partial Y_i}{\partial z}\right) - \frac{\partial v C_i}{\partial z} - \frac{(1-\varepsilon_b)}{\varepsilon_b}\frac{aK_{m,i}}{(Bi_{m,i}+1)}(C_i - \bar{c}_i) \tag{3}$$

where C_i is the concentration for a pure component in the bulk phase, D_{ax} is the axial dispersion coefficient for the *i*th component, Y_i is the mole fraction, v is the interstitial velocity, ε_b is the bed porosity, a is the pellet specific area, $K_{m,i}$ is the external mass transfer coefficient, and $Bi_{m,i} = R_p K_{m,i}/(5\varepsilon_p D_{p,i})$ is the mass Biot number.

Overall Mass Balance

The total mass balance equation was obtained adding up all the pure component mass balance equations with $i = 1, N$

$$\frac{\partial C}{\partial t} = -\frac{\partial v C}{\partial z} - \sum_{i=1}^{n}\frac{(1-\varepsilon_b)}{\varepsilon_b}\frac{aK_{m,i}}{Bi_{m,i}+1}(C_i - \bar{c}_i) \tag{4}$$

where C is the total gas concentration in the bulk phase.

Mass Balance Inside the Pellet

The mass balance inside the bidisperse porous particle yields the following Equation (31):

$$\frac{\partial \bar{c}_i}{\partial t} = \frac{15 D_{p,i}}{R_p^2}\frac{Bi_{m,i}}{(Bi_{m,i}+1)}(C_i - \bar{c}_i) - \frac{\rho_p}{\varepsilon_p}\frac{\partial \bar{\bar{n}}_i}{\partial t} \tag{5}$$

where $\bar{c}_i$ is the average mole concentration of the *i*th pure component inside

the pellet, $D_{p,i}$ is the pore diffusivity, ε_p is the pellet porosity, ρ_p is the pellet density and R_p is the pellet radius.

Mass Balance Inside the Crystal

$$\frac{\partial \bar{\bar{n}}_i}{\partial t} = \frac{15 D_{c,i}}{r_c^2}(\bar{n}_i^* - \bar{\bar{n}}_i) \tag{6}$$

where $\bar{n}_i{}^*$ is the equilibrium adsorbed concentration as a function of the average gas concentration inside the pores $\bar{c}_i$ and $\bar{\bar{n}}_i$ is the average adsorbed concentration of the single component i, with $D_{c,i}$ as the crystal diffusivity, and r_c the crystal radius.

Adsorption Equilibrium Model: Toth Multicomponent

The extension of Toth equation to multicomponent mixtures as suggested by Sircar (30) was implemented in the model.

$$\bar{n}_i^* = q_{m,i} \frac{b_i \bar{c}_i \Re T_s}{\left(1 + \sum_{i=1}^{N} (b_i \bar{c}_i \Re T_s)^k\right)^{1/k}} \tag{7a}$$

with

$$b_i = b_0 \exp\left(\frac{-\Delta H_i}{\Re T_s}\right) \tag{7b}$$

where $q_{m,i}$ is the saturation adsorption capacity for each component, b_i is the affinity constant for a specific sorbate, ΔH_i is the adsorption enthalpy for the ith component, $\Re$ is the ideal gas constant and T_s is the solid temperature. The extended Toth equation is used with a global heterogeneity parameter k. This parameter is different from the single parameter k_i used in the pure component Toth model. It is calculated from the single component isotherms with:

$$k = \sum_{i}^{N} y_i k_i \tag{7c}$$

Many different forms of the energy balance have been used in the mathematical description of non-isothermal adsorption processes, and various assumptions can be applied to simplify process simulations. Thus, in this study the temperature gradient in the radial direction has been neglected to describe a heterogeneous energy balance that takes into account three different control volumes (i.e., fluid- phase, solid and wall column).

Energy Balance for the Gas Phase

$$\frac{\partial T_g}{\partial t} = \frac{1}{\varepsilon_b C \tilde{C}_v} \frac{\partial}{\partial z}\left(\lambda \frac{\partial T_g}{\partial z}\right) - v \frac{\tilde{C}_p}{\tilde{C}_v} \frac{\partial T_g}{\partial z} + \frac{\Re T_g}{C \tilde{C}_v} \frac{\partial C}{\partial t} - \frac{(1-\varepsilon_b)}{\varepsilon_b} \frac{a h_f}{C \tilde{C}_v} (T_g - T_s) - \frac{2 h_w}{\varepsilon_b C \tilde{C}_v R_w} (T_g - T_w) \tag{8}$$

where λ is the axial heat dispersion coefficient, R_w is the column internal radius, $\tilde{C}_p$ and $\tilde{C}_v$ are respectively the molar specific heat of the bulk gas mixture at constant pressure and constant volume. The terms h_f and h_w are the heat transfer coefficient between the gas and the solid on the one hand, and between the gas and the wall, on the other hand.

Energy Balance for the Solid Phase

It is worth pointing out that the temperature inside the solid is considered as uniform. Thermal conduction in the solid phase and heat transfer between solid and wall phases are neglected.

$$\frac{\partial T_s}{\partial t} = \frac{(1-\varepsilon_b)\varepsilon_p \Re T_s}{B} \frac{\partial \bar{c}}{\partial t} + \frac{\rho_b}{B} \sum_{i=1}^{n} (-\Delta H_i) \frac{\partial \bar{\bar{n}}_i}{\partial t} + \frac{(1-\varepsilon_b) a h_f}{B} (T_g - T_s) \tag{9a}$$

with

$$B = (1-\varepsilon_b)\left\{\varepsilon_p \sum_{i=1}^{n} \bar{c}_i \tilde{C}_{v,i} + \rho_p \sum_{i=1}^{n} \partial \bar{\bar{n}}_i \tilde{C}_{v,ads,i} + \rho_p \hat{C}_{ps}\right\} \tag{9b}$$

where $\hat{C}_{ps}$ is the mass specific heat of the solid.

Wall Energy Balance

The wall conduction phenomenon is neglected.

$$\frac{\partial T_w}{\partial t} = \frac{1}{\rho_w \hat{C}_{pw}} \{\alpha_w h_w (T_g - T_w) - \alpha_{wl} U (T_w - T_\infty)\} \tag{10}$$

where $\hat{C}_{ps}$ is the mass specific heat of the wall column, ρ_w is the wall density, T_∞ is the temperature outside the column, and U is the overall heat transfer coefficient between the column wall and the external environment. The term α_w is the ratio of the internal surface area to the volume of the column wall, while α_{wl} is the ratio of the logarithmic mean surface area of the column shell to the volume of the column wall.

Variable Velocity of the Gas along the Bed

The variation of velocity of the bulk phase along the axial direction of the bed, $\partial v/\partial z$, is the result of the global mass and solid energy balances. Substituting Eq. (8) in Eq. (4), and applying the ideal gas law, the interstitial gas velocity can be written as follows

$$\frac{\partial v}{\partial z} = -\frac{1}{C}\sum_{i=1}^{n}\frac{(1-\varepsilon_b)}{\varepsilon_b}\frac{aK_{m,i}}{(Bi_{m,i}+1)}(C_i-\bar{c}_i) - \frac{(1-\varepsilon_b)}{\varepsilon_b} \frac{ah_f}{C\tilde{C}_p}\left(1-\frac{T_s}{T_g}\right) - \frac{2h_w}{\varepsilon_b C\tilde{C}_p R_w}\left(1-\frac{T_w}{T_g}\right) \tag{11}$$

Initial and Boundary Conditions

Since the adsorbent bed is filled with an inert gas, the initial conditions are:

$$t = 0, \forall z \quad C_i = \bar{c}_i = \bar{\bar{n}}_i = 0 \quad T_g = T_s = T_w = T_0 \quad v = v_0 \tag{12a}$$

Once the fixed bed column is saturated with an adsorptive flowing gas with mole fraction $Y_i = y_{i,0}$, the set of initial conditions related to the mass balance should be replaced by:

$$C_i = \bar{c}_i = \bar{\bar{n}}_i = y_{i,0} \tag{12b}$$

The Danckwert's boundary conditions are imposed at the inlet and outlet of the column for each gas mole fraction variable and gas-bulk temperature

$$z = 0 \quad -D_{ax}C\left.\frac{\partial Y_i}{\partial z}\right|_{z=0} + v(C_i - C_{i,0}) = 0 \quad \text{and}$$

$$-\frac{\lambda}{\varepsilon_b C\tilde{C}_v}\left.\frac{\partial T_g}{\partial z}\right|_{z=0} + v\frac{\tilde{C}_p}{\tilde{C}_v}(T_g - T_{g,0}) = 0 \tag{13}$$

$$z = L \quad \left.\frac{\partial Y_i}{\partial z}\right|_{z=L} = 0 \quad \text{and} \quad \left.\frac{\partial T_g}{\partial z}\right|_{z=L} = 0 \tag{14}$$

It should be mentioned that this mathematical model has been proposed following the work of Da Silva et al. (31). Further information and dimensionless model equations can be found elsewhere (26).

Determination of Model Parameters

The main drawback in using mathematical models for design and analysis of sorption system is that they require many input parameters, some of which could only be obtained using parameter estimation. Nevertheless, in the present study, most of the parameters were calculated from various correlations that have been widely used for column adsorption. Thus, the molecular diffusivities $D_{m,i}$ were calculated with the Chapman-Enskog equation using the Lennard-Jones parameters collected by Bird et al. (32) and listed in appendix (Table A1). For the calculation of the pore diffusivities, $D_{p,i}$, the Bosanquet equation has been applied:

$$\frac{1}{D_{p,i}} = \tau\left(\frac{1}{D_{m,i}} + \frac{1}{D_{k,i}}\right) \quad \text{with} \quad D_{k,i} = 97 r_p \sqrt{\frac{T}{M_i}} \tag{15}$$

where τ is the tortuosity factor assumed to be equal to 2.2, $D_{m,i}$ is the molecular diffusivity of the pure ith component and $D_{k,i}$ is the Knudsen diffusivity in $m^2 \cdot s^{-1}$. Note that the pore radius r_p is expressed in meter and the molecular weight of each gas, M_i, in g/mol.

For the crystal diffusivity $D_{c,i}$, the value of this parameter was directly taken from the data available in the literature (33, 34). In fact, intracrystalline diffusivities for alkanes and alkenes in 13X zeolite have been widely discussed and it has been shown, that the crystal diffusivities of the studied hydrocarbons decrease according to the following sequence: $C_3H_8 > C_3H_6 > C_4H_8$. The molar specific heat at constant pressure $\tilde{C}_{p,i}$ for the pure component i, was calculated by using the methods and thermodynamic data provided by Reid et al. (35) and reported in appendix (see Table A1). The molar specific heat at constant volume $\tilde{C}_{v,i}$ for each component was calculated from the $\tilde{C}_{p,i}$ using the ideal gas relationship $\tilde{C}_{v,i} = \tilde{C}_{p,i} - \Re$, where $\Re$ is the ideal gas constant. The thermal gas conductivity $k_{g,i}$ and the gas viscosity μ_i of each species were calculated according to the suggestions of Bird et al. (32). The external mass transfer coefficient $K_{m,i}$ and the heat convective coefficient h_f were estimated with the correlations of Wakao and Funazki (36):

$$K_{m,i} = \frac{Sh_i D_{m,i}}{2R_p} \tag{16}$$

and

$$h_f = \frac{N_u k_g}{2R_p} \tag{17}$$

Depending on the considered species, the Sherwood number Sh_i and the Nusselt number N_u ranged from 6 to 8 and from 7 to 9, respectively. To calculate both mass and heat axial dispersion coefficient D_{ax} and λ, the

correlations proposed by Wakao and Funazki (36) have been again used:

$$D_{ax} = \frac{D_{m,i}}{\varepsilon_b}(20 + 0.5Sc_iRe_i) \tag{18}$$

and

$$\lambda = k_g(7 + 0.5\mathrm{Pr}_iRe_i) \tag{19}$$

where Sc_i is the Schmidt number ($\mu_0/\rho_i D_{m,i}$), Re is the particle Reynolds number ($\rho_i v_s d_p/\mu_0$) and Pr is the Prandtl number ($\hat{C}_{pg}\mu_0/k_g$). For all the studied systems, Schmidt and Prandtl numbers were found to be around 0.6 and 0.9, respectively.

Finally, regarding the internal convective heat transfer coefficient h_w between the gas and wall column, the correlation proposed by Wasch and Froment (37) gave very high values ($>200\mathrm{W/m^2 \cdot K}$) which could not be used to correctly describe the temperature histories. The same was true for estimating the global heat transfer coefficient U with the correlation of Incropera and Witt (38) which led to unsatisfactory simulation results. Consequently, these two parameters were estimated on the experimental breakthrough curves.

Simulation Method

Various numerical techniques developed for the solution of the fixed bed adsorber model have been proposed in the literature. In the present work, orthogonal collocation on finite element has been applied to solve the system of partial differential equations (PDE), ordinary differential equations (ODE) and algebraic equations (AE) involved in the mathematical model. For the axial domain, 50 elements were used with 3 collocation points per element. The set of ordinary and algebraic equations (ODAE) were then integrated with the DASOLV solver which is based on backward-differentiation formulae (BDF). The absolute tolerance was fixed at 10^{-5} for all the simulations.

RESULTS AND DISCUSSION

Thermodynamics

Adsorption Isotherms of Pure Components on 13X Zeolite

The experimental equilibrium data of 1-butene on 13X zeolite measured at four temperatures (333, 353, 373, and 393 K) are listed in Table 2. Pressure P is given in kPa and the absolute amount adsorbed per unit mass of adsorbent q_i in mol/kg. The mean relative deviation calculated from Eq. (2) between experimentally measured amount adsorbed and their values obtained with the Toth model is

Table 2. Experimental data of 1-butene adsorption equilibrium on zeolite 13X

$T = 333$ K		$T = 353$ K		$T = 373$ K		$T = 393$ K	
P (kPa)	q (mol/kg)	P (kPa)	q (mol/kg)	P (kPa)	q (mol/kg)	P (kPa)	q (mol/kg)
0.00	0.000	0.00	0.000	0.00	0.000	0.00	0.000
0.75	1.650	0.10	0.903	2.10	1.267	0.30	0.534
5.60	1.858	0.50	1.396	5.60	1.460	2.40	1.063
21.45	1.966	2.75	1.580	11.05	1.617	9.40	1.419
29.20	1.992	10.00	1.757	14.95	1.675	20.25	1.602
39.55	2.011	18.95	1.824	23.20	1.733	26.70	1.648
48.10	2.023	34.85	1.885	34.15	1.774	33.75	1.684
56.05	2.031	47.05	1.911	42.50	1.790	52.45	1.736
66.10	2.039	61.15	1.936	56.10	1.823	67.50	1.764
76.10	2.047	73.60	1.950	71.20	1.865	76.30	1.778
86.05	2.052	82.15	1.962	82.85	1.881	85.05	1.797
100.50	2.057	98.80	1.973	94.60	1.900	102.90	1.816
108.20	2.060	107.25	1.981	108.05	1.922	110.05	1.827

found to be less than 2% for any temperature. The representative experimental data and the resulting fits from the Toth model are shown in Fig. 1. It can be seen in this figure that the experimental results of 1-butene on 13X zeolite are well correlated with the Toth isotherm. Fitted parameters are reported in Table 3. The isosteric heat of adsorption at zero coverage estimated with the Toth model is found to be 54.4 kJ/mol for 1-butene. This value is in good agreement with the sorption enthalpy measured by Malka-Edery et al. using a

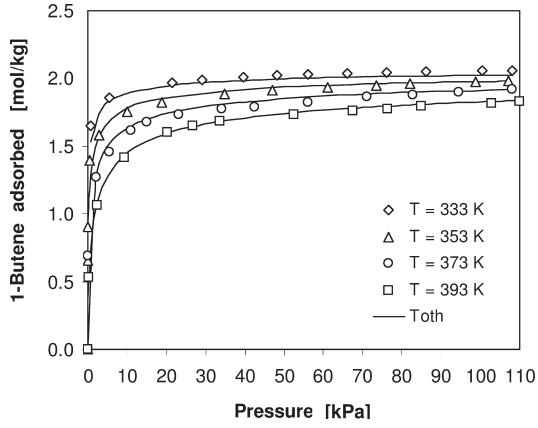

Figure 1. Equilibrium isotherms of 1-butene over 13X zeolite at different temperatures. The solid line is the Toth model.

Table 3. Adsorption equilibrium parameters of the Toth model on 13X zeolite

Gas	$q_{m,i}$ (mol/kg)	$b_{i,0}$ (kPa^{-1})	$-\Delta H_i$ (kJ/mol)	A_i (−)	D_i (K^{-1})
Propylene	2.59	2.5×10^{-7}	42.4	0.658	0.0
Propane	2.20	2.5×10^{-7}	36.9	0.892	0.0
1-Butene	2.10	2.5×10^{-7}	54.4	0.452	0.0

volume step thermal method (VSTM) (39). In their study, a mean sorption heat of 53 kJ/mol was found for anhydrous 13X zeolite.

In a previous work (26), propane and propylene isotherms on 13X zeolite were measured using the same experimental equipment and protocol as describe in this study.

Figure 2 shows the 373 K isotherms for propane (C_3H_8), propylene (C_3H_6) and 1-butene (C_4H_8) in the pressure range of 0 to 110 kPa. At low pressures the 1-butene isotherm exhibits the greatest slope and the highest adsorption capacity. The C_3H_8 and C_3H_6 isotherms have a more gradual slope at low pressure but continue to show increases in the amount adsorbed at pressure far greater than the value at which the C_4H_8 isotherm levels off. On the other hand, in this pressure range ($P \geq 20$ kPa), it can be observed that 1-butene isotherm is perfectly intermediate to the two C_3 component isotherms. This suggests that at 373 K the 1-butene can be a potential desorbent in the framework of a propane-propylene separation by SMB. Although this information is interesting, such a conclusion cannot be drawn only from single-adsorption isotherms.

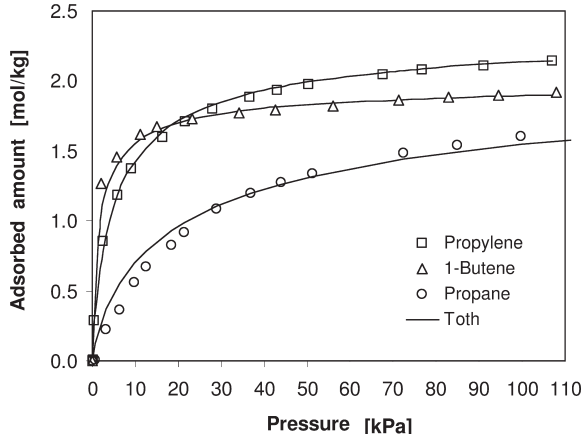

Figure 2. Comparison of pure gas adsorption isotherms on 13X zeolite at 373 K. The solid line is the Toth model.

Prediction of Binary Adsorption Equilibrium

The binary interaction of 1-butene with propane and propylene on 13X zeolite was investigated by simulation in order to get some insight into the real adsorption behavior of 1-butene in presence of the C_3 hydrocarbons. Thus, the isotherms parameters obtained from pure component equilibrium data were employed in the extended Toth model to predict the binary adsorption equilibria of both 1-butene/propane and 1-butene/propylene systems at 373 K and at the total pressure of 110 kPa. The model prediction for the binary adsorption equilibrium of C_4H_8/C_3H_8 mixture is shown in Fig. 3a. Because of the competitive adsorption between the two components, the amounts adsorbed of each species in the binary adsorption are different from those in the pure component adsorption. The total adsorbed amount of this binary mixture decreases slightly with propane composition increment as shown in Fig. 3a. This is because the equilibrium amount of 1-butene adsorbed is greater than the one of propane. Figure 3b shows the simulated binary adsorption equilibrium of 1-butene/propylene system. It can be seen from this figure that 1-butene is more selectively adsorbed than propylene. Another way to point out that 1-butene is preferentially adsorbed on 13X zeolite, is to calculate the selectivity factor defined as follows:

$$S_{A/B} = \frac{x_A/x_B}{y_A/y_B} \tag{20}$$

where x and y are the molar fractions of a component in the adsorbed phase and the gas phase, respectively (A is the stronger adsorbing component). Thus, a value of 3.84 is found for the C_4H_8/C_3H_6 system while 16.43 is obtained for the couple C_4H_8/C_3H_8. Finally, the last way to clearly show the affinity of the zeolite 13X for 1-butene adsorption in the presence of the C_3 components is to plot the simulated results of C_4H_8 mole fraction in the gas phase versus those in the adsorbed phase in a X-Y diagram for each system (Fig. 3c).

Dynamic Study

As noticed before from the simulations of binary equilibrium isotherms, the 1-butene is just slightly more easily adsorbed than the propylene and much more adsorbed than the propane. This is a first indication about the appropriateness of 1-butene to be a potential desorbent. Nonetheless, in order to confirm that 1-butene/zeolite 13X could be a promising couple to perform propane-propylene separation by SMB, it is essential to investigate the dynamics of adsorption and desorption of 1-butene in a fixed bed packed with 13X zeolite. Therefore, pure 1-butene breakthrough experiments were performed through an adsorbent bed initially activated with nitrogen. Then, the desorption of 1-butene was carried out by feeding the column with either pure propane or pure propylene until complete desorption. These

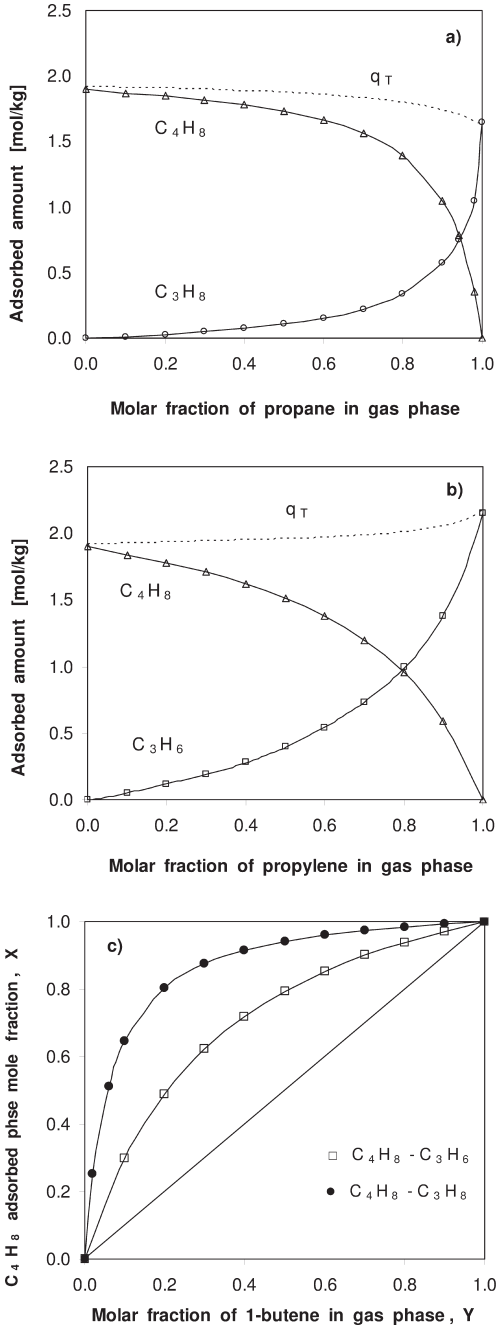

Figure 3. Simulations of binary adsorption equilibrium of a) 1-butene/propane system and b) 1-butene/propylene system over zeolite 13X at 373 K and 110 kPa. c) X-Y diagram for both systems predicted by the extended Toth model.

experiments allow to evaluate the ability of C_3 components to displace the desorbent (1-butene) from the zeolite. Subsequently, considering that the typical composition of an industrial gas mixture is 75% of C_3H_6 and 25% of C_3H_8, breakthrough and reverse breakthrough experiments were performed using 1-butene and this mixture. Finally, the set of breakthrough experiments is completed with a comparative study between 1-butene and isobutane which has been proposed in a previous work (26) as a convenient desorbent to displace both propane and propylene from a bed of zeolite 13X. All fixed bed experiments were carried out with a feed volumetric flowrate of 1.0 SLPM, at 373 K and 110 kPa. Table 4 provides further information regarding the experimental conditions. Note that all the adsorption breakthrough curves in this study are plotted in molar flowrate versus time.

Pure 1-Butene Adsorption on a 13X Zeolite Fixed Bed

Figure 4 shows a typical breakthrough curve of 1-butene over a fixed bed adsorbent initially filled with nitrogen at 110 kPa and 373 K. Also shown are the experimental and simulated temperature histories at the middle and top of the column (corresponding to the gas bulk temperature and wall temperature, respectively). The experimental breakthrough curves for single component were simulated using the model parameter values listed in Table 5, together with the physical properties given in appendix (Table A1). With regard to the overall heat transfer coefficient U, and the heat wall transfer coefficient h_w, the values found by fitting the simulation breakthrough curves to experimental data, range from 15 to 45 $W/m^2 \cdot K$, and are in good agreement with the ones reported in the literature (7). It is observed that the mathematical model proposed in the previous section, provides a good representation of the experimental breakthrough curves as well as the temperature histories.

For a quantitative comparison purpose, experimental and simulated adsorbed amount were calculated. For each experimental breakthrough

Table 4. Experimental conditions for the runs performed with 1-butene, propane, propylene and their mixtures

Run	Initial bed saturation	y_{C3H6}	y_{C3H8}	Y_{C4H8}	Q (SLPM)	P_0 (bar)	T_0 (K)	Figure
1	N_2	0.0	0.0	1.0	1.0	1.1	373	4a, 4b
2	C_4H_8	0.0	1.0	0.0	1.0	1.1	373	5a, 5b
3	C_4H_8	1.0	0.0	0.0	1.0	1.1	373	7a, 7b
4	C_3H_6-C_3H_8	0.0	0.0	1.0	1.0	1.1	373	9a, 9b
5	C_4H_8	0.75	0.25	0.0	1.0	1.1	373	10a, 10b
6	C_3H_6	0.0	0.50	0.50	1.0	1.1	373	12a, 12b

Note: Q is the volumetric flow in SLPM at standard conditions (273.15 K, 1.01325 10^5 Pa).

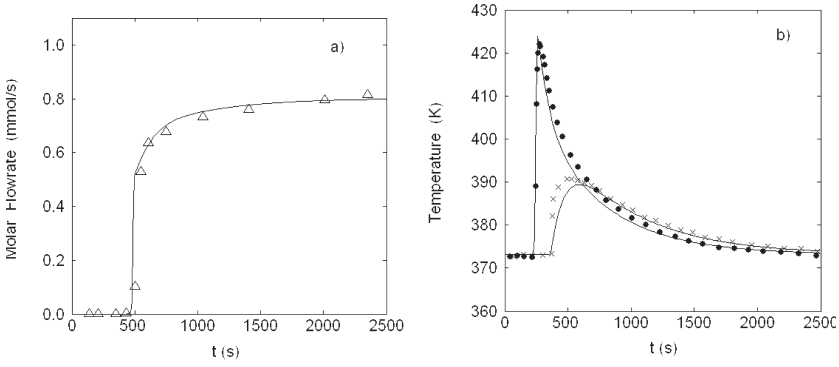

Figure 4. Typical adsorption breakthrough curve of pure 1-butene (△) on 13X zeolite at the bed exit; b) gas temperature histories at the middle bed (•) and wall column temperature histories at the top bed (×) during the adsorption of 1-butene. Solid lines are simulations obtained with the non-isothermal bidisperse model. ($Q = 1.0$ SLPM; $P = 1.1$ bar; $T = 373$ K).

curve, the adsorbed amount was calculated as follows:

$$q_i = \frac{1}{\rho_p(1-\varepsilon_b)V_c}\int_0^{\infty}(F_0 - F_i)dt - \frac{\varepsilon_b}{\rho_p(1-\varepsilon_b)}\frac{F_0}{Q_0} \tag{21}$$

where ρ_p is the pellet density, ε_b is the bed voidage fraction, V_c is the volume of the column occupied by the solid adsorbent, Q_0 is the feed volumetric flowrate, and F_0 is the feed molar flowrate. The evolution of F_i at the bed exit is taken into

Table 5. Calculated parameters used in the simulations

Parameters	C_3H_6	C_3H_8	C_4H_8	Unit
Mass parameters				
ρ_i	1.49	1.56	1.99	$kg \cdot m^{-3}$
D_c (33, 34)	$2.69\ 10^{-11}$	$4.42\ 10^{-11}$	$2.10\ 10^{-11}$	$m^2 \cdot s^{-1}$
D_p	$5.74\ 10^{-6}$	$5.45\ 10^{-6}$	$4.52\ 10^{-6}$	$m^2 \cdot s^{-1}$
D_{ax}	$10.49\ 10^{-4}$	$9.98\ 10^{-4}$	$8.46\ 10^{-4}$	$m^2 \cdot s^{-1}$
K_m	$4.61\ 10^{-2}$	$4.44\ 10^{-2}$	$3.97\ 10^{-2}$	$m \cdot s^{-1}$
B_i	5.04	5.11	5.51	—
Energy parameters				
k_g	$3.34\ 10^{-2}$	$2.77\ 10^{-2}$	$2.85\ 10^{-2}$	$W \cdot m^{-1} \cdot K^{-1}$
λ	0.47	0.39	0.47	$W \cdot m^{-1} \cdot K^{-1}$
h_f	101.6	85.8	99.0	$W \cdot m^{-2} \cdot K^{-1}$
$\tilde{C}_{p,i}$	89.33	76.40	103.0	$J \cdot mol^{-1} \cdot K^{-1}$
$\tilde{C}_{v,i}$	81.02	68.08	94.68	$J \cdot mol^{-1} \cdot K^{-1}$

Note: parameters calculated at the feed conditions (373 K, 1.1 bar and $u_0 = 0.06$ $m \cdot s^{-1}$).

Table 6. Experimental and simulated adsorbed amount

Run	Initial bed saturation	y_{C3H6}	y_{C3H8}	y_{C4H8}	q_{C3H6} (mol/kg)		q_{C3H8} (mol/kg)		q_{C4H8} (mol/kg)	
					Exp.	Sim.	Exp.	Sim.	Exp.	Sim.
1	N_2	—	—	1.0	—	—	—	—	2.028	1.913
2	C_4H_8	—	1.0	0.0	—	—	0.554	0.602	1.042	1.091
3	C_4H_8	1.0	—	0.0	2.142	2.168	—	—	1.864	1.905
4	C_3H_6-C_3H_8	0.0	0.0	1.0	1.872	1.864	0.119	0.118	1.997	1.909
5	C_4H_8	0.75	0.25	0.0	1.834	1.860	0.117	0.115	1.985	1.902
6	C_3H_6	0.0	0.50	0.50	2.134	2.188	0.065	0.062	1.765	1.758

account in the calculation, which was measured experimentally. The experimental and theoretical adsorbed concentrations are shown in Table 6. It can be observed that discrepancies between experimental and predicted adsorbed amount are not significant. Furthermore, the experimental adsorbed concentration measured at 373 K and 110 kPa by gravimetric method is in good agreement with the adsorbed concentration estimated from breakthrough curves.

Desorption of Pure 1-Butene: Pseudo-Binary Breakthrough Curves

The term "pseudo-binary breakthrough curve" as used in this study means a single component breakthrough curve which has been performed in a fixed bed initially saturated with an adsorptive species. Thus, the behavior of the two pure components can be investigated during the same run, one being desorbed by the adsorption of the other. Here, the main idea was to observe desorption of 1-butene by passing either pure propane or propylene in the fixed bed.

The displacement of 1-butene by the adsorption of propane is shown in Fig. 5a. Desorption breakthrough curve of 1-butene is very broad. This tailing is due to a large extent to the adsorption isotherm of 1-butene that is highly favorable compared to the one of propane in a binary mixture (see Fig. 3c). Although the desorption is not entirely accomplished experimentally, it can be assumed according to the experimental curve shape, that the time required to complete the desorption of 1-butene with propane will be longer (more than 3000 sec. by simulations). The variation of bulk phase velocity along the column is an important aspect that was taken into account in this work. Figure 5b shows the superficial velocity history at the column outlet.

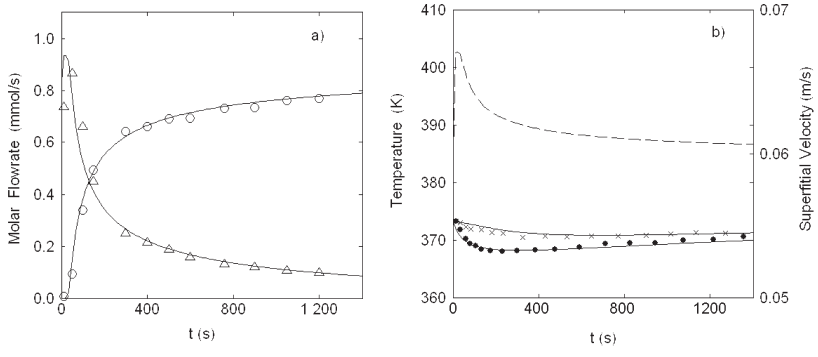

Figure 5. Experimental breakthrough curves of propane (○) on 13X zeolite initially saturated with 1-butene (△); b) gas temperature histories at the middle bed (•) and wall column temperature histories at the top of the bed (×) during the adsorption of pure propane. Solid lines are simulations of molar flowrate and temperature breakthrough curves. Dashed line represents the variation of superficial velocity predicted by the model ($Q = 1.0$ SLPM; $P = 1.1$ bar; $T = 373$ K).

Looking at the temperature history at the bed outlet on Fig. 5b, we can see that the range of thermal variations is quite small (less than 5°C).

Looking at the outlet velocity history on Fig. 5b, we can see a roll-up phenomenon. Since temperature variations are small, as it can also be observed from the gas temperature bed profiles (Fig. 6c), this velocity variation should be explained by another phenomenon. In fact, looking at the evolution with time of the adsorbed quantity profile in the bed on Fig. 6b, we can see that this quantity decreases with time due to the difference of adsorbed capacity between 1-butene and propane. So there is more desorbed 1-butene than adsorbed propane. This is the reason why we can see on Fig. 6a that the superficial velocity is higher when and where the adsorbed quantity is high: there is a desorbed 1-butene flow which is just partially balanced by the adsorbed

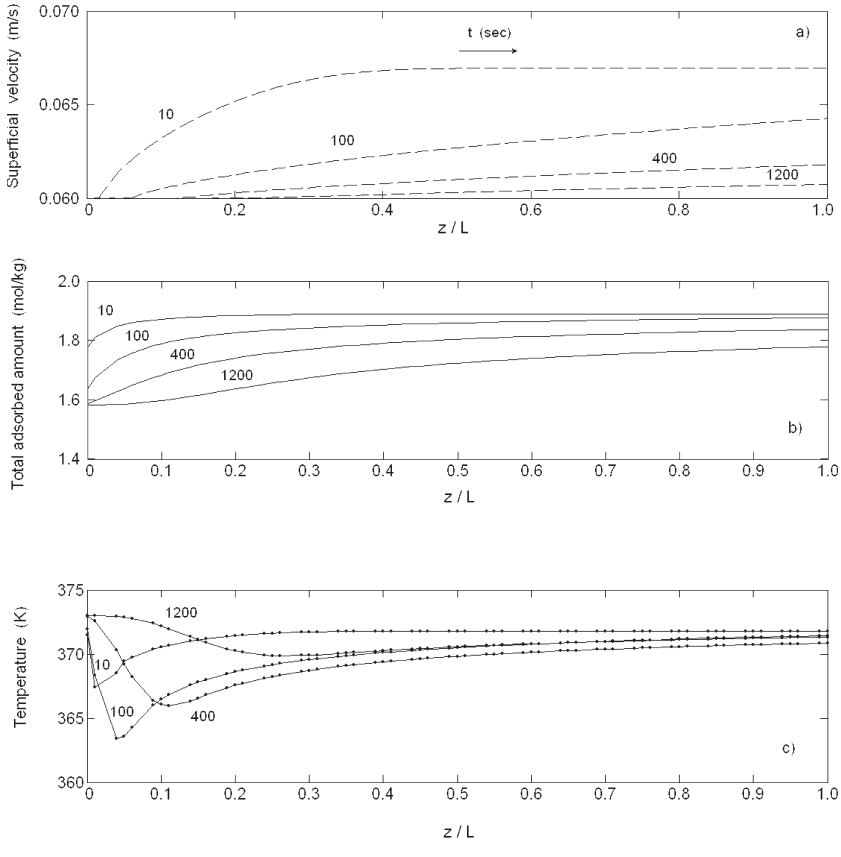

Figure 6. a) Superficial velocity axial profiles at different times b) bed profiles of the total adsorbed amount and c) bed profiles of gas temperature during the adsorption of pure propane over 13X zeolite initially saturated with 1-butene at 373 K and 110 kPa.

propane flow, and the difference between the desorbed and the adsorbed flows is added to the bulk flow resulting in a higher superficial velocity.

This velocity peak leads to a typical roll up in the 1-butene wave desorbed by the propane. This establishes the fact that the effect of velocity variation is particularly significant and is the main cause of roll over phenomenon. Considering the temperature histories, a significant thermal well is noted, due to the smaller heat of adsorption of propane in comparison with the one measured for 1-butene (36.9 kJ/mol and 54.4 kJ/mol, respectively).

Figure 7 shows the adsorption of propylene through a fixed bed fully saturated with 1-butene. One can observe that the exit molar flowrate breakthrough curves of propylene adsorption and 1-butene desorption are dispersive. This is a consequence of the favorable adsorption isotherm of 1-butene when it is involved in a binary mixture with propylene (as can be seen in Fig. 3c). These observations are in agreement with the equilibrium theory, which predicts dispersive concentration fronts in the case of the desorption of a component with a favorable isotherm. Regarding the gas and wall column temperature histories, it can be observed that the system is almost isothermal. This is a consequence of an energy compensation between the energy necessary for the propylene adsorption and the one released during the desorption of 1-butene. In fact, multiplying the heat of adsorption of propylene by its loading at the feed condition, a value of $+110$ kJ/kg is found, while the energy discharged per kilogram of adsorbent during the desorption of 1-butene is around -114 kJ/kg. These values are very close and explain the very low thermal sink. In the same way, it should be noticed that superficial velocity along the bed is almost constant and no roll up is observed in the breakthrough curves. It is worth noting that in both cases, modeling results compare very well with the experimental breakthrough data (see Table 6).

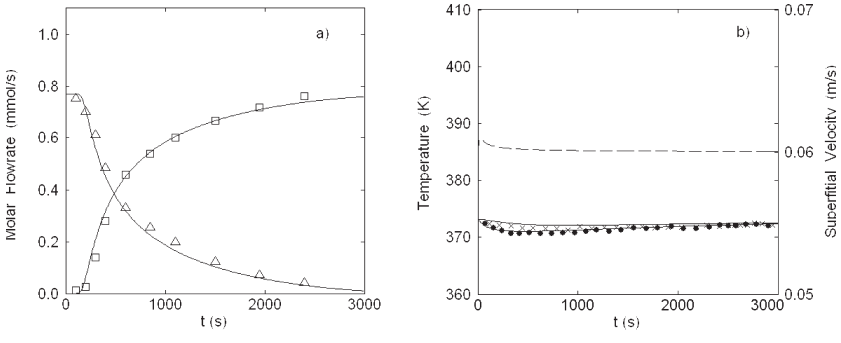

Figure 7. a) Experimental breakthrough curves of propylene (□) on 13X zeolite initially saturated with 1-butene (△); b) gas temperature histories at the middle bed (•) and wall column temperature histories at the top of the bed (×) during the adsorption of pure propylene. Solid lines are simulations of molar flowrate and temperature breakthrough curves. Dashed line represents the variation of superficial velocity ($Q = 1.0$ SLPM; $P = 1.1$ bar; $T = 373$ K).

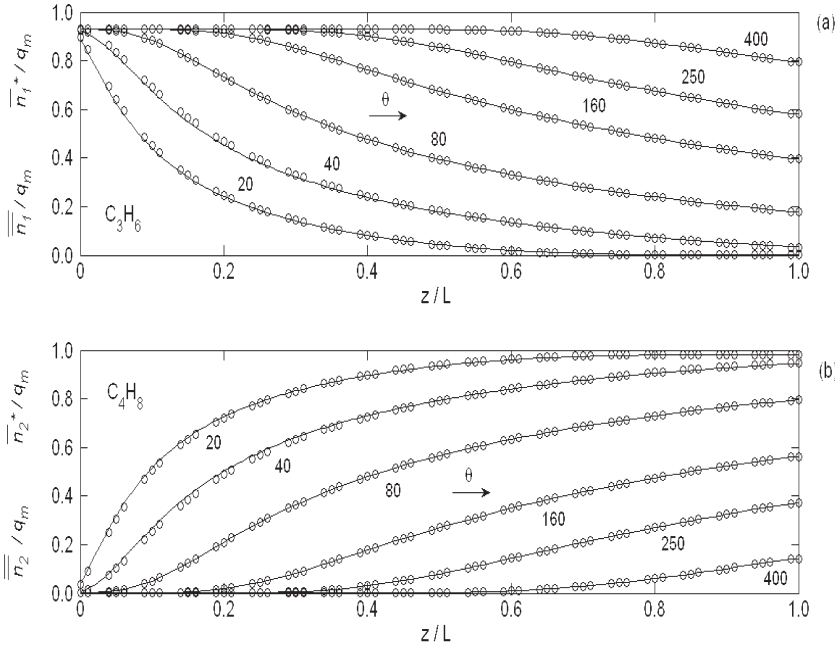

Figure 8. Simulated dimensionless concentration profile in adsorbed phase (solid lines) and dimensionless equilibrium solid concentration (○○○) along the adsorption fixed bed at different dimensionless times θ. (a) Propylene adsorption at 373 K and 1.1 bar ($Q = 1.0$ SLPM), (b) 1-butene desorption at the same operating conditions.

Figure 8 shows the bed profiles of dimensionless adsorbed phase concentration $\bar{\bar{n}}_i/q_{m,i}$ and the values obtained at equilibrium with the macroporous phase $\bar{\bar{n}}_i^*/q_{m,i}$ at different dimensionless times ($\theta = u_0 t/\varepsilon_b L$) for propylene adsorption and 1-butene desorption, respectively. It is observed that dimensionless adsorbed solid concentration (solid lines) and the respective equilibrium values (circles) are markedly the same. Therefore, considering this simulation, it can be concluded that the macropore resistance is higher than micropore resistance. Another way to demonstrate that macropore mass transfer is the controlling mechanism is to use Ruthven and Loughlin criterion (40, 41), written as:

$$\gamma = \frac{(D_c/r_c^2)(1+K)}{(D_p/R_p^2)} \tag{22}$$

where $K = (1-\varepsilon_p)H/\varepsilon_p$ is the capacity factor and H the slope of the considered isotherm at the origin. Macropore diffusion is the controlling mechanism for $\gamma > 10$, while for $\gamma < 0.1$ the micropore diffusivity is the dominant mass transfer mechanism. For both gases, we found $\gamma > 700$. This result confirms the previous conclusion made from the simulations regarding the macropore control.

Counter-Diffusion of 1-Butene and Propane/Propylene Mixture

The purpose of the following fixed bed experiments is to evaluate the suitability of 1-butene as a desorbent for the regeneration of 13X zeolite when it is fully saturated with a propane-propylene mixture. Figure 9 shows the breakthrough curves and temperature histories of 1-butene adsorption over a fixed bed adsorbent originally saturated with a propane (25%)/propylene (75%) mixture. It can be clearly observed that 1-butene readily displace the gas mixture from the adsorbent. As stated previously through the adsorption phase diagram (Fig. 3c), the adsorption isotherm of 1-butene is highly favorable compared to the ones of the C_3 components; therefore the breakthrough curves are sharp with well distinguishable plateaus and abrupt transitions. Breakthrough time is rather short, the adsorbent bed being fully regenerated in less than 1200 sec. A relevant velocity variation is markedly noted on breakthrough curves. In this experiment, temperature histories present a small thermal peak due to the high adsorption enthalpy of 1-butene compared with propane adsorption heat. On the other hand, the reverse breakthrough experiment shown in Fig. 10, reveals that the displacement of the selected desorbent by adsorption of propane-propylene mixture is difficult in view of the dispersive fronts and the long time required to achieve a complete desorption of 1-butene. Thus, although the desorbent is able to easily displace the adsorbed C_3 hydrocarbons from 13X zeolite, the reverse operation is more difficult to carry out, 1-butene being in strong interaction with the adsorbent and impeding propane-propylene adsorption.

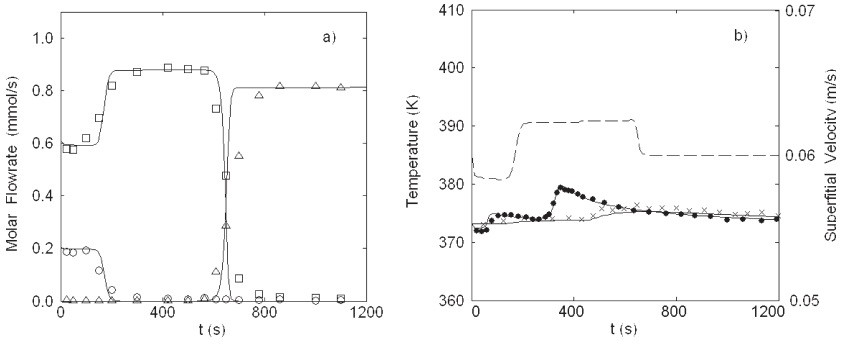

Figure 9. a) Blowdown curves of propylene/propane mixture on 13X zeolite by adsorption of 1-butene; b) gas temperature histories at the middle of the bed (•) and wall column temperature histories at the top of the bed (×) during the desorption of the mixture. (□) Propylene, (○) Propane and (△) 1-butene. Solid lines are simulated molar flowrate and temperature breakthrough curves obtained with the non-isothermal bidisperse model. Dashed line is the superficial velocity variation at the bed outlet. (feed composition: 75% propylene – 25% propane $Q = 1.0$ SLPM; $P = 1.1$ bar; $T = 373$ K).

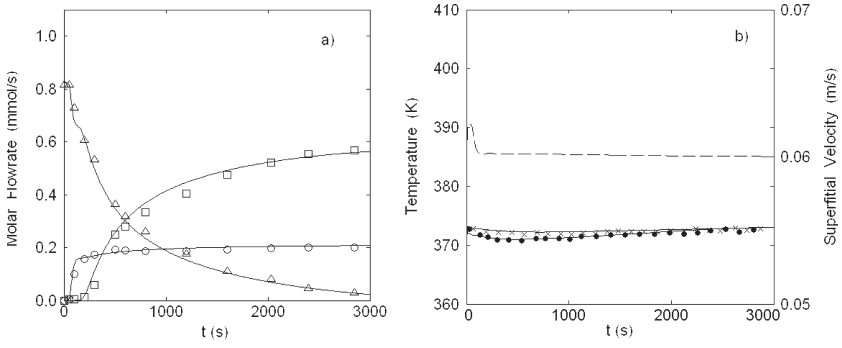

Figure 10. a) Adsorption breakthrough curves of propylene/propane mixture on 13X zeolite initially saturated with 1-butene; b) gas temperature histories at the middle of the column (•) and wall column temperature histories at the top of the bed (×) during the adsorption of the mixture. (□) Propylene, (○) Propane and (△) 1-butene. Solid lines are simulated molar flowrate and temperature breakthrough curves obtained with the non-isothermal bidisperse model. Dashed line is the superficial velocity variation at the bed outlet. (feed composition: 75% propylene – 25% propane $Q = 1.0$ SLPM; $P = 1.1$ bar; $T = 373$ K).

The small disparities between experimental and simulated breakthrough curves can be reduced by taking into account the pressure drop along the equipment. Although this problem has not been examined here in details, it can easily be solved by adding the momentum balance to the model.

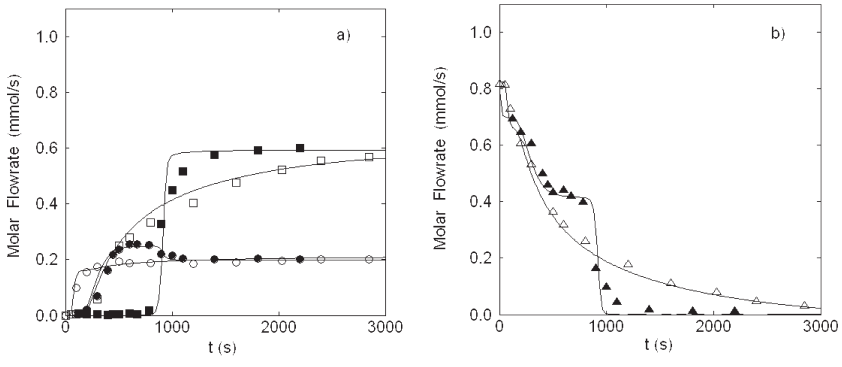

Figure 11. Comparison of 1-butene and isobutane as desorbent for the displacement of propylene/propane mixture. a) Both adsorption of propylene/propane mixture over a bed initially saturated with 1-butene (□ Propylene, ○ Propane) and isobutane (■ Propylene, • Propane), respectively. b) Both desorption of 1-butene (△) and isobutane (▲) during the adsorption of propylene/propane mixture. Solid lines are simulations obtained with the model (feed composition: 75% propylene – 25% propane $Q = 1.0$ SLPM; $T = 373$ K).

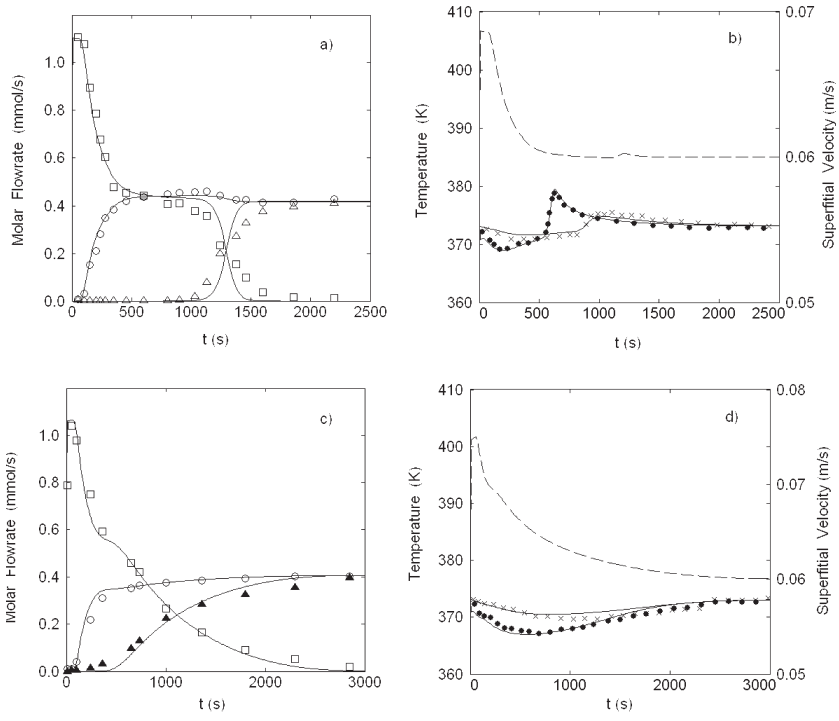

Figure 12. Comparison of 1-butene (△) and isobutane (•) in presence of propane (○) and propylene (□) a) Breakthrough curves of 1-butene/propane mixture on 13X zeolite initially saturated with propylene (feed composition: 50% 1-butene – 50% propane; $Q = 1.0$ SLPM; $P = 1.1$ bar; $T = 373$ K) ; c) Breakthrough curves of isobutane/propane mixture on 13X zeolite initially saturated with propylene (feed composition: 50% isobutane – 50% propane; $Q = 1.0$ SLPM; $P = 1.5$ bar; $T = 373$K) ; b)–d) gas temperature histories at the middle bed (•) and wall column temperature histories at the top of the bed (×) during the adsorption of the mixtures. Dashed line represents the superficial velocity variation at the bed outlet.Solid and dashed lines are simulations obtained with the non-isothermal bidisperse model.

Nevertheless, the model proposed in this study, provides good predictions of multicomponent breakthrough curves.

1-Butene and Isobutane as Desorbent: A Comparative Study

In a previous work (26), adsorption of isobutane on 13X zeolite was studied as a desorbent to displace both propane and propylene from a bed of zeolite 13X. In this part, results obtained with isobutane are compared to those obtained with 1-butene.

For comparison purpose, adsorption/desorption breakthrough curves of 1-butene and isobutane have been studied in terms of ability to displace a

typical propane-propylene mixture from zeolite 13X. Figure 11a shows a comparison of binary breakthrough curves for adsorption of propane-propylene mixture (25/75) in a fixed-bed adsorbent initially saturated either with isobutane (black marks) or 1-butene (white marks). In the case of isobutane, the breakthrough curves of the gas mixture are shaper than the ones resulting from an adsorbent bed originally filled with 1-butene. In the same way, it can be observed in Fig. 11b that desorption breakthrough curve of 1-butene exhibits more tailing and is broader than isobutane desorption profile. These results are attributed to the nature of the desorbent isotherm, which is favorable for 1-butene and unfavorable for isobutane in a mixture involving propylene. According to the equilibrium theory, for a system with an unfavorable isotherm since in desorption, compressive concentration waves are expected. In addition, from this figure it can be deduced the following selectivity sequences for the two systems considered in this study:1-butene >propylene > propane and propylene > isobutane > propane.

Further fixed bed experiments were performed in order to confirm these selectivity sequences and above all to compare the adsorption of both 1-butene and isobutane in presence of C_3 hydrocarbons. Thus, in Fig. 12 are presented adsorption breakthrough curves of equimolar mixtures of propane/1-butene and propane/isobutane through a fixed bed adsorbent initially saturated with propylene. In both cases the bed preferentially adsorbs the desorbent from the mixture. Mass fronts are more compressive with a mixture involving 1-butene than the one comprising isobutane. So, it can be concluded that 1-butene is a promising desorption agent, especially for displacing propane-propylene mixture from 13X zeolite in a SMB process.

CONCLUSION

In this work, 1-butene has been studied as a potential desorption agent over zeolite 13X for C_3 olefin/paraffin separation. It has been shown that 1-butene was able to easily displace both adsorbed propane and propylene from the 13X zeolite packed in a fixed-bed column. We also observed that 1-butene was held rather strongly by the zeolite, making the loading up of the adsorbent difficult with a propane-propylene mixture. The mathematical model including a double LDF approximation for the mass transfer, a heterogeneous energy balance, and a variable velocity of the gas phase through a fixed-bed column packed with bidisperse porous particles, has been formulated and gave an excellent prediction of the experimental breakthrough curves.

The present work may be considered as first steps in the modelling of a simulated moving bed for the separation of propane-propylene mixture. In addition, the experimental information provided can be applied for the successful design and operation of such a process. Two potential desorbent/adsorbent couples have been clearly identified:1-butene/13X zeolite and isobutane/13X zeolite

NOTATION

a	pellet specific area
b	adsorption equilibrium constant (-)
Bi	Biot number (-)
C	total fluid phase concentration (mol/m^3)
C_i	concentration of i component is the bulk phase (mol/m^3)
$\bar{c}_i$	average concentration of i component inside the pellet pores (mol/m^3)
$\tilde{C}_p$	molar specific heat at pressure constant of the gas mixture (J/mol · K)
$\tilde{C}_{pw}$	wall specific heat (J/kg ·K)
$\tilde{C}_v$	molar specific heat at volume constant of the gas mixture (J/mol · K)
D_{ax}	mass axial dispersion coefficient (m^2/s)
D_c	crystal diffusion coefficient (m^2/s)
D_m	molecular diffusivity (m^2/s)
D_p	pore diffusivity (m^2/s)
F_i	molar flow rate of i component is the bulk phase (mol/s)
ΔH_i	isosteric heat of adsorption of i component (J/mol)
h_f	film heat transfer coefficient between gas and solid (W/m^2 · K)
h_w	film heat transfer coefficient between gas and the wall (W/m^2 ·K)
k_g	gas thermal conductivity (W/m · K)
K_m	mass transfer coefficient (m/s)
L	length of the column (m)
M	molecular weight (g/mol)
$\bar{\bar{n}}_i$	average adsorbed concentration for i component in the pellet (mol/kg)
$\bar{n}_i^*$	adsorbed phase concentration in the crystal in equilibrium with the gas inside the particule (mol/kg)
P	gas pressure (Pa)
Q	volumetric flow rate (SLPM)
q_m	maximum loading capacity of the sorbent (mol/kg)
q_T	total adsorbed amount (mol/kg)
$\Re$	ideal gas constant (=8.3143 J/mol · K)
r_c	crystal radius (m)
r_p	pore radius (m)
R_p	pellet radius (m)
t	time variable (s)
T_g	gas temperature (K)
T_s	solid temperature (K)
T_w	wall temperature (K)
T_∞	temperature outside the column (K)
U	overall heat transfer coefficient (W/m^2 · K)
u	superficial velocity (m/s)
v	interstitial velocity (m/s)

Greek Letters

ε_b	bulk porosity $(-)$
ε_p	pellet porosity $(-)$
λ	heat axial dispersion coefficient $(W/m \cdot K)$
η	viscosity $(Pa \cdot s)$
ρ_b	bulk density (kg/m^3)
ρ_p	pellet density (kg/m^3)
θ	dimensionless time $(-)$

Superscripts

*	equilibrium
$-$	volumetric average
$=$	double volumetric average
$\sim$	per mole

Subscripts

c	crystal
g	gas
i	species
o	reference feed condition
p	pellet; constant pressure
s	solid
v	constant volume
w	wall

Abbreviations

LDF	Linear driving force
MSB	Magnetic suspension balance
OCFEM	Orthogonal collocation in finite elements method
ODAE	Ordinary differential and algebraic equations
ODE	Ordinary differential equations
PDAE	Partial differential and algebraic equations
PDE	Partial differential equation
PSA	Pressure swing adsorption
SMB	Simulated moving bed

APPENDIX

Table A1. Physical properties of propylene, propane, 1-butene and isobutane

						$\tilde{C}_{p,i} = \sum_{i=0}^{3} A_i T^i$(J/mol · K)			
Gas	M_i (g/mol)	σ (Å)	ε/κ (K)	T_c (K)	P_c (bar)	A_0	A_1	A_2	A_3
C_3H_6	42.08	4.766	275	365.0	46.1	3.71	$2.35\ 10^{-1}$	$-1.16\ 10^{-4}$	$2.21\ 10^{-8}$
C_3H_8	44.10	4.934	273	369.8	42.5	−4.22	$3.01\ 10^{-1}$	$-1.60\ 10^{-4}$	$3.22\ 10^{-8}$
C_4H_8	56.11	4.536	276	414.0	40.2	−2.99	$3.53\ 10^{-1}$	$-1.99\ 10^{-4}$	$4.46\ 10^{-8}$
iC_4H_{10}	58.12	5.393	295	408.1	36.5	−1.39	$3.85\ 10^{-1}$	$-1.85\ 10^{-4}$	$2.89\ 10^{-8}$

ACKNOWLEDGMENTS

The authors acknowledge financial support from the Institut Français du Pétrole (IFP). N.L. gratefully acknowledges the grant from Association Nationale de la Recherche Technique (Research fellowship: CIFRE 518/2004).

REFERENCES

1. Manley, D.B. and Swift, G.W. (1971) Relative volatility of propane-propene system by integration of general coexistence equation. *J. Chem. Eng. Data*, 16 (3): 301.
2. Bryan, P.F. (2004) Removal of propylene from fuel-grade propane separation and purification review 33 (2): 157–182.
3. Eldridge, R.B. (1993) Olefin/paraffin separation technology: a review. *Ind. Eng. Chem. Res.*, 32 (10): 2208.
4. Ghosh, T.K., Lin, H.-D., and Hines, A.L. (1993) Hybrid adsorption-distillation process for separating propane and propylene. *Ind. Eng. Chem. Res.*, 32 (10): 2390.
5. Kumar, R., Golden, T.C., White, T.R., and Rokicki, A. (1992) Novel adsorption distillation hybrid scheme for propane/propylene separation. *Sep. Technol.*, 15: 2157.
6. Safarik, D.J. and Eldridge, R.B. (1998) Olefin/paraffin separations by reactive absorption: A Review. *Ind. Eng. Chem. Res.*, 37: 2571.
7. Da Silva, F.A. and Rodrigues, A.E. (2001) Propylene/propane separation by VSA using 13X zeolite. *AIChE J.*, 47 (2): 341–357.
8. Da Silva, F.A. and Rodrigues, A.E. (2001) Vacuum swing adsorption for propylene/propane separation with 4A zeolite pellets. *Ind. Eng. Chem. Res.*, 40 (24): 5758–5774.
9. Rege, S.U. and Yang, R.T. (2002) Propylene/propane separation by PSA: sorbent comparison and multiplicity of cyclic steady states. *Chem. Eng. Sci.*, 57: 1139–1149.
10. Grande, C.A. and Rodrigues, A.E. (2005) Propane/propylene separation by pressure swing adsorption using zeolite 4A. *Industrial & Engineering Chemistry Research*, 44: 8815–8829.
11. Broughton, D.B. and Gerhold, C.G.. Continuous Sorption Process Employing Fixed bed of Sorbent and Moving Inlets and Outlets. U.S. Patent 2,985,589, 1961.
12. Ruthven, D.M. and Ching, C.B. (1989) Countercurrent and simulated countercurrent adsorption separation processes. *Chem. Eng. Sci.*, 44: 1011.
13. Yang, R.T. (1997) *Gas Separation by Adsorption Processes*; Imperial College Press: London, U.K.
14. Storti, G., Mazzotti, M., Furlan, L.T., Morbidelli, M., and Carra, S. (1992) Performance of a six port simulated moving bed pilot plant for vapor-phase adsorption separations. *Sep. Sci. Tech.*, 27: 1889.
15. Mazzotti, M., Storti, G., and Morbidelli, M. (1997) Optimal operation of simulated moving bed units for nonlinear chromatographic separations. *J. Chrom. A.*, 3: 769.
16. Cheng, L.S. and Wilson, S.T.. Process for Separating Propylene from Propane. U.S. Patent 6,293,999 B1, September 25, 2001.

17. Rao, D.P., Sivakumar, S.V., and Ramaprasad, B.S.G. (2005) Novel simulated moving-bed adsorber for the fractionation of gas mixtures. *Journal of Chromatography A*, 1069 (1): 141–51.
18. Mota, J.P.B., Esteves, I.A.A.C., and Eusébio, M.F.J. (2007) Synchronous and asynchronous SMB process for gas separation. *AIChE J.*, 53 (5): 1192–1203.
19. Grande, C.A. and Rodrigues, A.E. (2004) Adsorption kinetics of propane and propylene in zeolite 4A. *Chemical Engineering Research and Design*, 82: 1604–1612.
20. Patino-Iglesias, M.E., Aguilar-Armenta, G., Jimenez-Lopez, A., and Rodriguez-Castellon, E. (2004) Kinetics of the total and reversible adsorption of propylene and propane on zeolite 4A (CECA) at different temperatures. *Colloids and Surfaces A*, 237 (2): 73–77.
21. Da Silva, F.A. and Rodrigues, A.E. (1999) Adsorption equilibria and kinetics for propylene and propane over 13X and 4A zeolite pellets. *Ind. Eng. Chem. Res.*, 38: 2051–2057.
22. Järvelin, H. (1994) Separation of propane and propylene. *Acta Polytech. Scandinavia Chem. Tech.*, 222: 1.
23. Järvelin, H. and Fair, J.R. (1993) Adsorptive separation of propylene-propane mixtures. *Ind. Engr. Chem. Res.*, 32 (10): 2201.
24. Järvelin, H. (1990) *Adsorption of Propane and Propylene;* Tech. Rep. SRP Doc., No. F-90-4, Separation Reasearch Program. The University of Texas: USA.
25. Grande, C.A., Araújo, J.D.P., Cavenati, S., Firpo, N., Basaldella, E., and Rodrigues, A.E. (2004) New π-complexation adsorbents for propane-propylene separation. *Langmuir*, 20: 5291–5297.
26. Lamia, N., Wolff, L., Leflaive, P., Sà Gomes, P., Grande, C.A., and Rodrigues, A.E. (2007) Propane/Propylene separation by simulated moving bed I. Adsorption of propane, propylene and isobutane in pellets of 13X zeolite. *Sep. Sci. and Tech.*, 42: 2539–2566.
27. Rodrigues, A.E., Lamia, N., Grande, C.A., Wolff, L., Leflaive, P., and Leinekugelle-Coq, D.. Procédé de Séparation du Propylène en Mélange avec du Propane par Adsorption en Lit Mobile Simulé en Phase Gaz ou Liquide utilisant une Zéolithe de type Faujasite 13X comme Solide Adsorbant. FR. Patent pending 06-06827, July, 2006.
28. Do, D.D. (1998) *Adsorption Analysis: Equilibria and Kinetics*; Series on Chemical Engineering; Imperial College Press: London, U.K.
29. Toth, J. (1971) State equations of the solid-gas interface layers. *Acad. Sci. Hung.*, 69 (3): 311.
30. Sircar, S. (1991) Role of adsorbent heterogeneity on mixed gas adsorption. *Ind. Eng. Chem. Res.*, 30: 1032.
31. Da Silva, F.A., Silva, J.A.C., and Rodrigues, A.E. (1999) A general package for the simulation of cyclic adsorption processes. *Adsorption*, 5: 229–244.
32. Bird, R.B., Stewart, W.E., and Lightfoot, E.N. (1960) *Transport Phenomena*, 2nd Edn; John Wiley and Sons, Inc.: New York.
33. Brandani, S., Hufton, J., and Ruthven, D.M. (1995) Self-diffusion of propane and propylene in 5A and 13X zeolite crystals studied by the tracer ZLC method. *Zeolites*, 15: 624–631.
34. Germanus, A., Kärger, J., and Pfeifer, H. (1984) Self diffusion of paraffins and olefins in Zeolite NaX under the influence of residual water molecules. *Zeolites*, 4: 188.
35. Reid, R.C., Prausnitz, J.M., and Poling, B.E. (1987) *The Properties of Gases and Liquids*, 4thEdn; McGraw-Hill: New York.

36. Wakao, N. and Funazkri, T. (1978) Effect of fluid dispersion coefficients on particle-to-Fluid mass transfer coefficients in packed beds. *Chem. Eng. Sci.*, 33: 1375–1384.
37. Wasch, A.P. D. and Froment, G.F. (1972) Heat transfer in packed beds. *Chem. Eng. Sci.*, 27: 567–576.
38. Incropera, F.P. and Witt, D.P. D. (1996) *Fundamentals of Heat and Mass Transfer*, 4th Edn.; John Wiley and Sons, Inc.: New York.
39. Malka-Edery, A., Abdallah, K., Granier, PH., and Meunier, F. (2000) Influence of traces of water on adsorption and diffusion of hydrocarbons in NaX zeolite. *Adsorption*, 7: 17–25.
40. Ruthven, D.M. and Loughlin, K.F. (1972) The diffusional resistance of molecular sieve pellets. *Can. J. Chem. Eng.*, 28: 550–552.
41. Silva, J.A.C. and Rodrigues, A.E. (1996) Analysis of ZLC technique for diffusivity measurements in bidisperse porous adsorbent pellets. *Gas. Sep. Purif.*, 10 (4): 207–224.